

Investigation of an F-18 oxytocin receptor selective ligand via PET imaging



Aaron L. Smith^{a,b}, Sara M. Freeman^b, Ronald J. Voll^a, Larry J. Young^{b,*}, Mark M. Goodman^{a,*}

^a Department of Radiology and Imaging Sciences, Emory University, Atlanta, GA 30329, United States

^b Center for Translational Social Neuroscience, Department of Psychiatry and Behavioral Sciences, Yerkes National Primate Research Center, Atlanta, GA 30322, United States

ARTICLE INFO

Article history:

Received 15 May 2013

Revised 12 July 2013

Accepted 22 July 2013

Available online 30 July 2013

Keywords:

Oxytocin

Oxytocin receptor

Receptor imaging

Fluorine-18

PET imaging

Cerebral ventricles

Choroid plexus

Alpha-1 adrenergic receptor

Adrenergic receptor

ABSTRACT

The compound 1-(1-(2-(2-(2-fluoroethoxy)-4-(piperidin-4-yloxy)phenyl)acetyl)piperidin-4-yl)-3,4-dihydroquinolin-2(1H)-one (**1**) was synthesized and positively evaluated in vitro for high potency and selectivity with human oxytocin receptors. The positron emitting analogue, [F-18]**1**, was synthesized and investigated in vivo via PET imaging using rat and cynomolgus monkey models. PET imaging studies in female Sprague–Dawley rats suggested [F-18]**1** reached the brain and accumulated in various regions of the brain, but washed out too rapidly for adequate quantification and localization. In vivo PET imaging studies in a male cynomolgus monkey suggested [F-18]**1** had limited brain penetration while specific uptake of radioactivity significantly accumulated within the vasculature of the cerebral ventricles in areas representative of the choroid plexus.

© 2013 Published by Elsevier Ltd.

Oxytocin was the first endocrine system hormone to be synthesized in the laboratory, and has been studied extensively for its role in the induction of labor and the milk ejection reflex.¹ More recently, research foci have been directed toward the role of oxytocin and the oxytocin receptor (OTR) in the regulation of psychosocial behavior.^{2–10} In addition to being implicated in modulating maternal nurturing and mother–infant bonding, pair bonding, social recognition, increased eye-to-eye contact, trust and empathy, the oxytocin system has also been investigated in relation to disorders characterized by disruption in social behavior, including autism spectrum disorders.^{11–17} While the bulk of the research conducted with the oxytocin system in humans has been limited to experimental paradigms involving administration of oxytocin followed by behavior monitoring, methodologies implemented for investigating OTR within the brain have been limited to post-mortem receptor autoradiography, in situ hybridization, and gene association studies.^{12,13,18–21} The development of a methodology permitting the quantification of OTR in the living brain would represent a significant advance in this area of research. Our goal is to develop a positron-emitting small molecule with high affinity and selectiv-

ity for the human and primate OTR to enable non-invasive correlations between neural OTR densities and behavior via in vivo positron emission tomography (PET). In addition to this goal, we are simultaneously seeking to discover new candidate pharmaceuticals which may prove useful in reaching OTR specifically within the brain or the periphery for the purpose of potentially alleviating and/or investigating symptoms associated with social behavior disorders. We report here the synthesis, radiosynthesis, and PET imaging evaluation of one of our lead candidate compounds meeting these criteria.

We have recently reported progress in the development of OTR selective ligands bearing radioactive isotopes with some bearing structural similarity to the lead candidate described here.^{22,23} These molecules were found to either not penetrate the blood–brain barrier or have high affinity for the p-glycoprotein pump which prevented their retention within the brain. We concluded that the lack of a hydrogen bond donor may have been the cause for lack of brain penetration or retention. Therefore, we proceeded to modify the structure by eliminating the methyl sulfonyl group of our former lead candidate, **2**, to generate a compound bearing a free amine to act as a hydrogen bond donor, **1** (Fig. 1). The synthetic route was derived from a precursor in our previously reported synthetic pathway, **3**, and is outlined in Scheme 1²² The free amine of **3** was protected using di-*tert*-butyl dicarbonate to generate **4**. The phenol position of **4** was then alkylated using

* Corresponding authors. Tel.: +1 (404) 727 8272; fax: +1 (404) 727 8070 (L.J.Y.). Tel.: +1 (404) 727 9366; fax: +1 (404) 712 5689 (M.M.G.).

E-mail addresses: lyoun03@emory.edu (L.J. Young), mgoodma@emory.edu (M.M. Goodman).

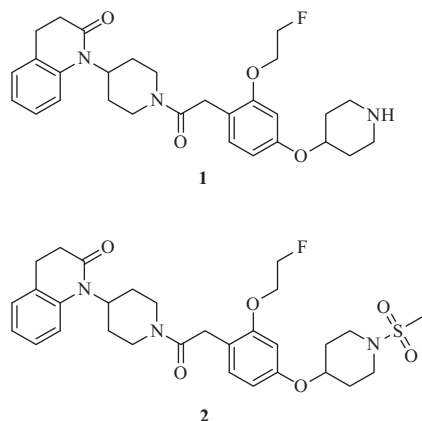
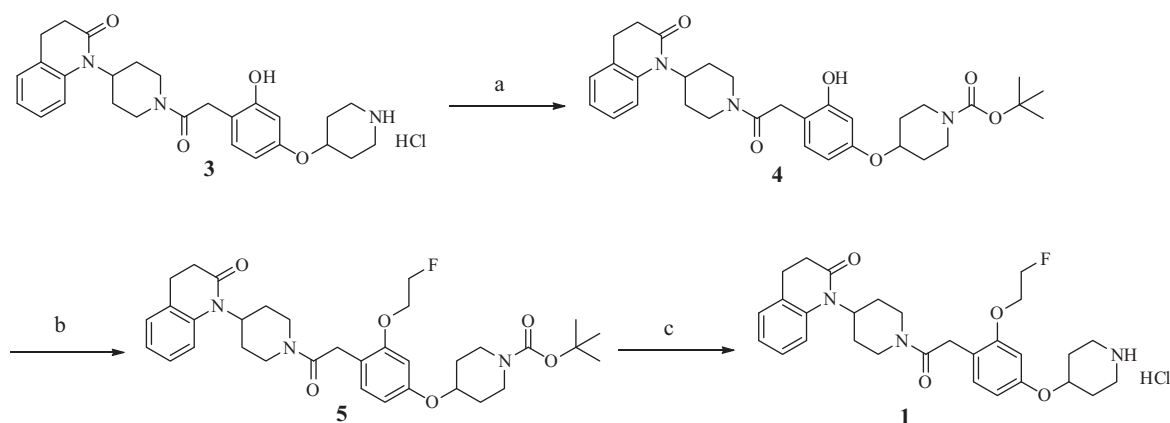


Figure 1. Structures of OTR selective compounds **1** and **2**.



Scheme 1. Synthetic route to obtain the target molecule **1**. Reagents and conditions: (a) Boc_2O , dioxane, 1 N NaOH, rt, 48%; (b) 1-bromo-2-fluoroethane, Cs_2CO_3 , DMF, rt, 97%, (c) (1) 2 M HCl in ether, rt, 96%. Further reaction details and characterizations are provided in the [Supplementary data](#).

1-bromo-2-fluoroethane to provide the fluoroethoxy moiety of **5**. A deprotection using 2 M HCl in ether then resulted in the target molecule, **1**, as a hydrochloride salt. Further synthetic details and characterizations are provided in the [Supplementary data](#).

To determine if the structural modification resulted in any loss of biological properties, **1** was subjected to in vitro competitive binding assays using cell lines expressing human oxytocin and all known vasopressin receptor subtypes (V1aR, V1bR, and V2R). The results of these assays are displayed in [Table 1](#) with data for **2** obtained from our previously reported study.²² These data indicate the removal of the methyl sulfonyl group actually resulted in a slight improvement of the biological properties. Having a K_i value of 15 nM for the OTR, **1** matched the binding affinity of **2**. While

Table 1

In vitro K_i (nM) determinations of **1–2** from competition assays with human OTR and vasopressin receptors (3 subtypes)^a

Compound	OTR	V1aR	V1bR	V2R
2	16	8700	>10,000	1800
1	15	5600	>10,000	8700

For experimental details please refer to the PDSP web site <http://pdsp.med.unc.edu/> and click on 'Binding Assay' or 'Functional Assay' on the menu bar.

^a K_i Values were generously provided by the National Institute of Mental Health's Psychoactive Drug Screening Program, contract # HHSN-271-2008-00025-C (NIMH PDSP). The NIMH PDSP is directed by Bryan L. Roth MD, PhD at the University of North Carolina at Chapel Hill and Project Officer Jamie Driscoll at NIMH, Bethesda MD, USA.

the binding affinity of **1** for the V1aR slightly increased, the binding affinity for the V2R decreased significantly in comparison to **2**, thus making it slightly more selective overall. Further in vitro binding assays were also performed on 88 other human G-protein coupled receptors (GPCR) in a screen to determine if **1** had affinity for these other receptors. [Table 2](#) contains the results of the screen in which 7 other GPCR had modest to mild affinity for **1**, none of which would be expected to display significant uptake during a PET scan. The most notable binding affinity was found in the alpha-1A subtype of the adrenergic receptor and the 6 subtype of the 5-hydroxytryptophan receptor (5-HT6) having a K_i values of 82 nM and 187 nM, respectively. Although these K_i values for the non-target receptors are not believed to be optimal for PET imaging, they would present an issue if **1** was to be considered for pharmaceutical development.

Having good binding affinity and selectivity, the F-18 analogue

of **1** was generated for further investigation. The synthetic route to [¹⁸F]**1** is outlined in [Scheme 2](#). The Boc-protected amine **4** was alkylated with ethane-1,2-diyl bis(4-methylbenzenesulfonate) to generate our tosylate precursor **6**. Radiolabeling was then conducted in a CTI-Seimens Chemistry process Control Unit (CPCU) to perform $\text{S}_{\text{N}}2$ substitution using the cryptand ligated $\text{K}_{222}^{18}\text{F}$ followed by removal of the Boc-protecting group with 1 M HCl. The crude radioactive mixture was eluted from the CPCU unit with a 7 ml solution of ethanol:water:triethylamine (50:50:0.1). Solid phase extraction was then performed to remove excess acid prior to HPLC purification. The extracted mixture was then purified via HPLC and concentrated into a dose form (15 ml solution of 10% ethanol in saline) via solid phase extraction and passed through 1 and 0.2 μm filters using high argon pressure. A dose would normally be prepared in 120 min from the start of synthesis and result in approximately 19% uncorrected yields of [¹⁸F]**1** with a specific activity greater than 10 Ci/ μmol . Radiochemical purity was greater than 99.9%. A representative analytical HPLC graph is shown in [Figure 2](#).

To gauge the probability of brain penetration, the log $P_{7,4}$ was determined to be 1.57 using previously reported methods. This lipophilicity measurement is within the range of 1–3 estimated to be the calculated optimal range for penetration of the blood brain barrier.²⁴ To evaluate brain penetration in vivo, PET studies were first performed using female 180–200 g Sprague–Dawley rats ($n = 4$) in the same manner as our previously reported study.^{22,25} [Figure 3](#) contains representative time activity curves generated

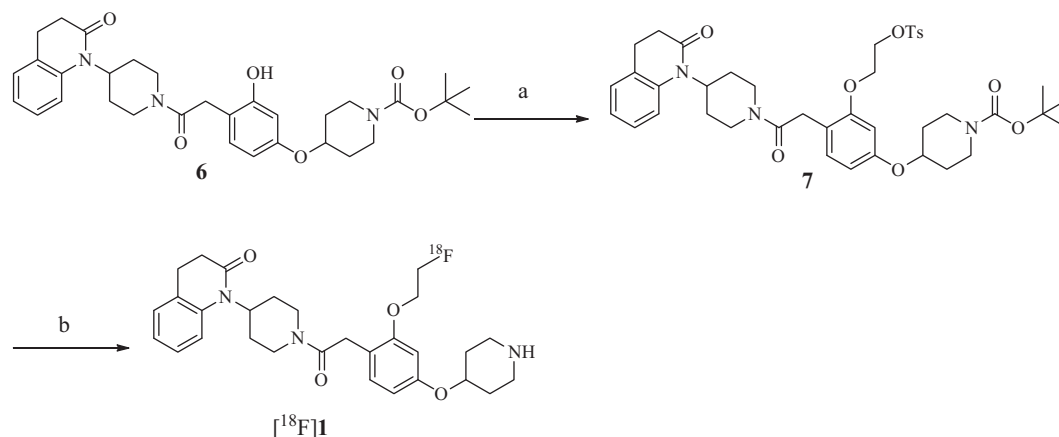
Table 2

In vitro K_i (nM) determinations of **1** from competition assays with the human muscarinic acetylcholine receptor (M4), the 1B, 2B, B, and 6 subtypes of the 5-hydroxytryptophan receptors (5-HT), the alpha 1A adrenergic receptor, and dopamine D3 receptor^a

Receptor	M4	5-HT1B	5-HT2B	5-HTB	5-HT6	Adrenergic alpha 1A	Dopamine D3
K_i (nm)	1270	700	500	1270	190	80	6790

For experimental details please refer to the PDSP web site <http://pdsp.med.unc.edu/> and click on 'Binding Assay' or 'Functional Assay' on the menu bar.

^a K_i Values were generously provided by the National Institute of Mental Health's Psychoactive Drug Screening Program, contract # HHSN-271-2008-00025-C (NIMH PDSP). The NIMH PDSP is directed by Bryan L. Roth MD, PhD at the University of North Carolina at Chapel Hill and Project Officer Jamie Driscoll at NIMH, Bethesda MD, USA.



Scheme 2. Synthetic route for obtaining [¹⁸F]**1**. Reagents and conditions: (a) ethane-1,2-diyl bis(4-methylbenzenesulfonate), Cs₂CO₃, DMF, rt, 55%; (b) (1) K₂₂₂¹⁸F, CH₃CN, 110 °C, 15 min; (2) 1 N HCl, 110 °C, 10 min, 19% (uncorrected). Further reaction details and characterizations are provided in the Supplementary data.

from [¹⁸F]**1** distribution which compares the muscle tissue uptake with whole brain uptake. As can be seen in the graph, there is a burst of activity into the brain at the beginning of the scan which clears after 20 min post injection. Therefore, the first 20 min of the scan were summed to analyze brain uptake. Figure 4 contains representative images of [¹⁸F]**1** over the first 20 min time span post injection. Uptake appears to be located at areas in and around the cerebral ventricles. However, it is difficult to make a conclusive determination of the exact areas of uptake in the rat due to the size of the subject, small areas of OTR binding in the rat brain, limits of resolution of the PET scanner, and limited time of retained uptake.

To further evaluate [¹⁸F]**1** in a model which would better represent a human and should be large enough to detect regions of OTR binding with a PET scanner, PET imaging was conducted using [¹⁸F]**1** in a cynomolgus monkey model. Three types of studies were performed to evaluate the tracer and its distribution within the brain, a baseline scan in which only the tracer was injected, a blocking scan (5 mg/kg of the cold standard was administered 30 min prior to the tracer), and a chase scan (5 mg/kg of cold standard was administered 45 min after the tracer). These procedures were performed on a subject anesthetized with Telazol (3 mg/kg; i.m.) and maintained on a 1–2% isoflurane in pure oxygen mixture while intubated and placed on a ventilator throughout the imaging procedure. A 15 min transmission scan was performed using a germanium-68 point source to provide attenuation correction. Approximately 5 mCi of [¹⁸F]**1** was then administered at the start of the emission scan and scanning continued for 2 h. For blocking and chase studies, 5 mg/kg of **1** was administered 30 min prior to [¹⁸F]**1** injection or 45 min after [¹⁸F]**1** injection, respectively, via a slow bolus injection.

Figure 5a–c contains images obtained from the sum of the 2 h baseline scan and arrows indicate the uptake found primarily in the ventricles within the brain. One possible site of radiotracer binding within the ventricles is the choroid plexus, which is a highly vascularized network of structures within the ventricles of

the brain which synthesizes and recycles cerebrospinal fluid (CSF). The time activity curves of the standard uptake values (SUV) for the ventricular lining, the whole brain, and the muscle tissue obtained from the baseline scan are shown in Figure 6a. The graph suggests significant amounts of [¹⁸F]**1** reach the brain during the first 500 s of the scan, but as can be seen by the concentration of [¹⁸F]**1** in the ventricular lining during the same timeframe, it could be deduced to account for the bulk of brain activity detected. Therefore, no significant accumulation of the ligand was detected in any sites within the brain. Thus, it could be deduced that [¹⁸F]**1** did not penetrate the extracellular space of the brain, and only reached the vasculature and the choroid plexus. As can be seen in Figure 5d which sums up the first 15 min of the scan, there is uptake observed at the middle cerebral artery in the sulcus of the outer region of the cerebral cortex near the insula. This may explain the increase in whole brain uptake during the first 500 s of the scan, although we cannot rule out accumulation in the CSF of this region. The time activity curve of the choroid plexus/ventricular lining in Figure 5a clearly demonstrates that [¹⁸F]**1** binds strongly in this area. Although there have been reports of vasopressin 1a and alpha-1A adrenergic receptors in this region, there are have been no reports of OTR in the choroid plexus.²⁶

To verify if the observed [¹⁸F]**1** uptake was due to binding to a saturable protein on the cerebral ventricles, blocking and chase scans were performed in which 5 mg/kg of the cold standard, **1**, was administered 30 min prior to [¹⁸F]**1** (blocking) or 45 min post injection of [¹⁸F]**1** (chase). The comparable time–activity curves are shown in Figure 6b and c, respectively. The blocking study resulted in an increase of overall brain activity, primarily in the region of the choroid plexus. The images obtained were nearly identical to those obtained from the baseline scan and are not shown. The observed increase of [¹⁸F]**1** after blocking is thought to be due to the blocking of peripheral OTR and perhaps the mild affinity **1** has for the alpha-1 adrenergic receptor (there is a vast distribution of these type of receptors in the periphery). Once the majority of

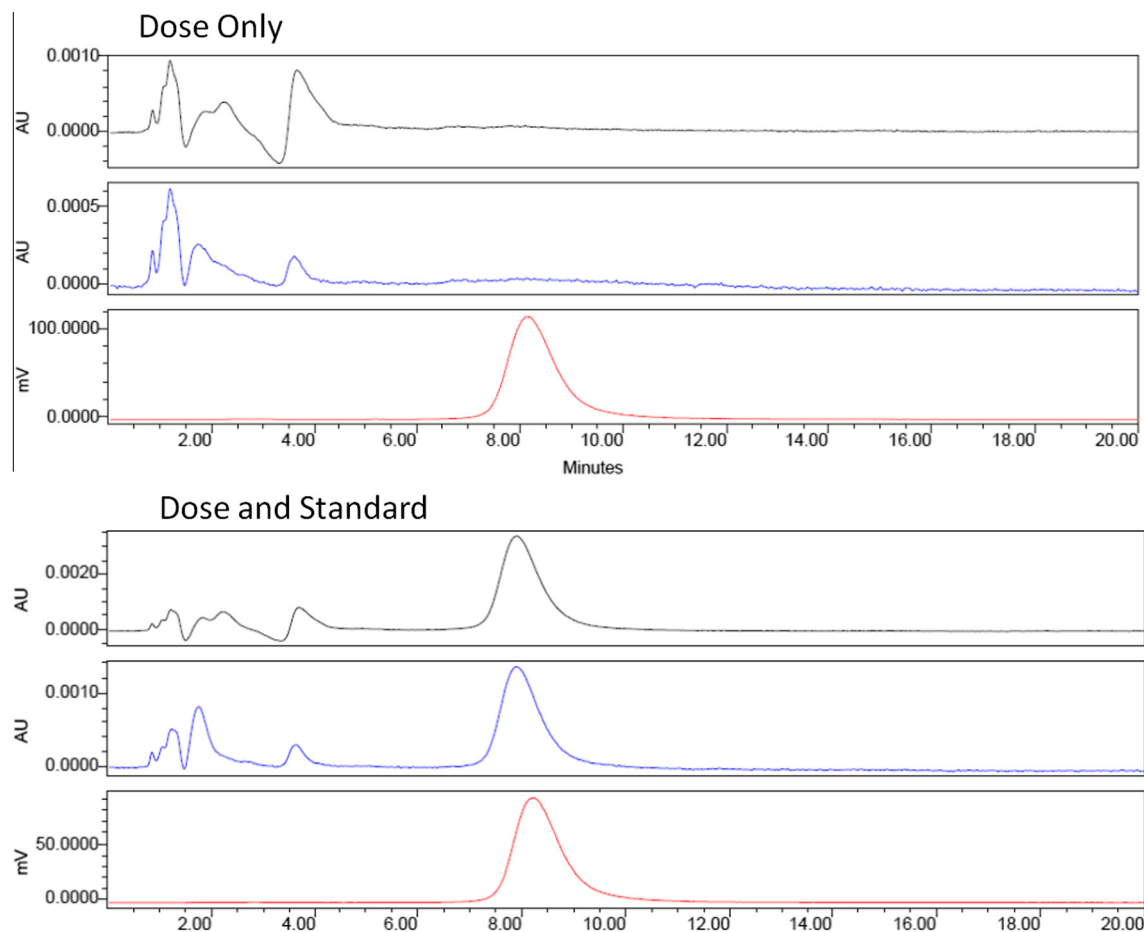


Figure 2. Two representative analytical HPLC chromatograms (dose and dose co-injected with cold standard) as obtained from a Waters Breeze HPLC system equipped with a Bioscan radiation detector and Novapak 4 μm C-18 column (3.9×150 mm). The chromatograms are showing graphs at 254 nm (top graph), 280 nm (middle graph) and detected radiation on the SAT/IN channel (bottom graph) by elution with a solution of methanol:water:triethylamine (70:30:0.1).

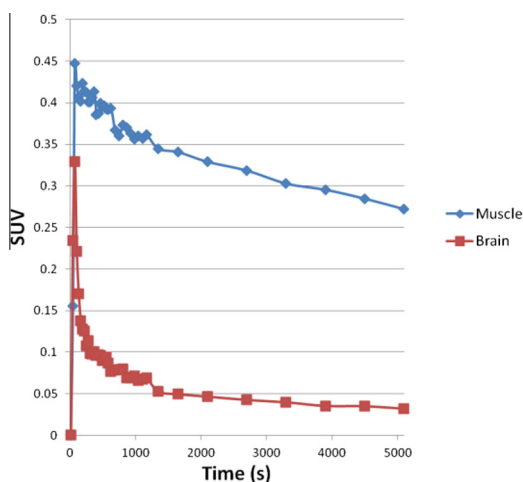


Figure 3. Baseline time-activity curves of the muscle tissue and brain generated from [^{18}F]**1** in a female Sprague Dawley rat model.

these receptors are blocked in the periphery, it allowed more tracer to become available in the blood, thus increasing the overall activity concentrations in the choroid plexus and vasculature. The inability of **1** to block the uptake of [^{18}F]**1** in the choroid plexus would suggest that the uptake is not specific to a saturable protein. However, the chase study afforded completely opposite results. In

the chase study, the uptake within the choroid plexus was completely removed after administration of **1** by the end of the remaining hour and 15 min of scan time. When the summed images from the final 30 min of both the baseline and chase scans are directly compared (Fig. 7), it is clearly evident [^{18}F]**1** is completely removed by the addition of **1**. These results suggest that **1** has some type of affinity equilibrium within the choroid plexus that shifts when additional amounts of **1** are administered. It should be noted that previously investigated PET imaging studies using pharmaceutical derivatives, including our studies with a completely different OTR selective molecule, have shown to have uptake in the choroid plexus region; the phenomenon is not unique to **1**.^{23,27,28}

In summary, a very selective OTR ligand, **1**, has been investigated in vitro with receptor binding assays and in vivo via synthesis of its positron emitting analogue, [^{18}F]**1**, and PET. Brain penetration of [^{18}F]**1** may be present in the rat, but appears to be limited to the choroid plexus area in both the cynomolgus macaque and the rat. In the cynomolgus monkey, brain penetration appears to be negligible except for specific uptake within the choroid plexus. Neither PET scan suggested [^{18}F]**1** will be useful for detecting OTR in vivo. It is possible that the densities of OTR in the cynomolgus monkey model are not high enough to afford a signal via PET using a biomarker with a K_i affinity greater than 1 nM, or that they even do not exist. Indeed, to date, inconclusive results have been reported regarding specific OTR binding in the rhesus macaque brain²⁹ (Young, LJ and Freeman, SM unpublished data). By contrast, we and others have confirmed that the common marmoset

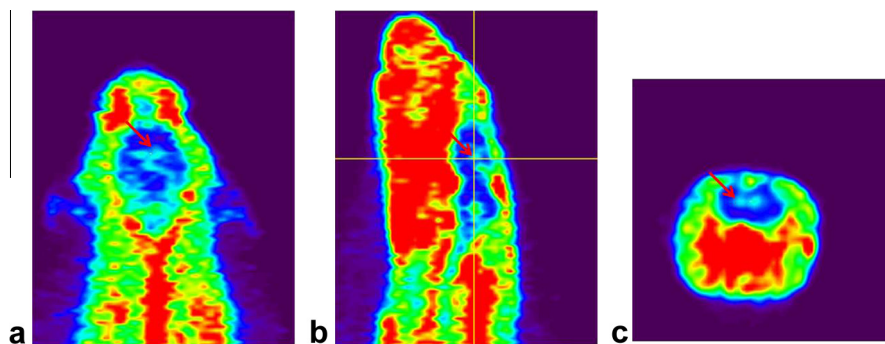


Figure 4. Representative images of 280 μCi of $[^{18}\text{F}]\mathbf{1}$ during the first 20 min of a PET scan with arrows pointing to the choroid plexus area in each image and the crosshairs of the sagittal image designating the slice locations of the coronal and transverse slices. (a) Transverse slice. (b) Sagittal slice. (c) Coronal slice.

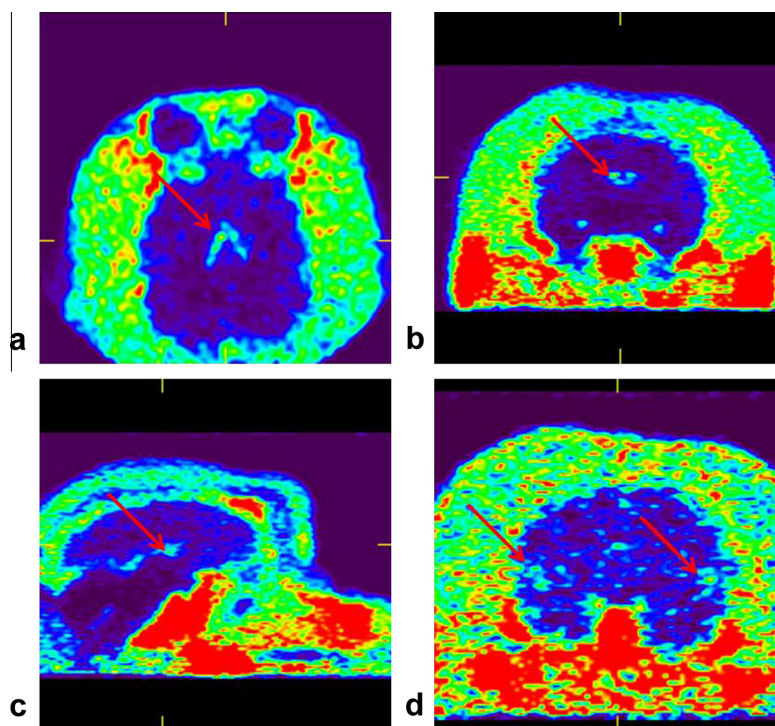


Figure 5. Images a–c were obtained from the sum of a 2 h scan of 5.5 mCi $[^{18}\text{F}]\mathbf{1}$ in a cynomolgus monkey model with arrows indicating uptake in the choroid plexus. (a) Transverse view at the lateral ventricle. (b) Coronal view at the lateral ventricle and inferior horn of lateral ventricle. (c) Sagittal view at the lateral ventricle. Image d was obtained from a sum of the first 15 min of the scan with arrows indicating $[^{18}\text{F}]\mathbf{1}$ at the middle cerebral artery within a sulcus of the outer cerebral cortex of the brain near the insula.

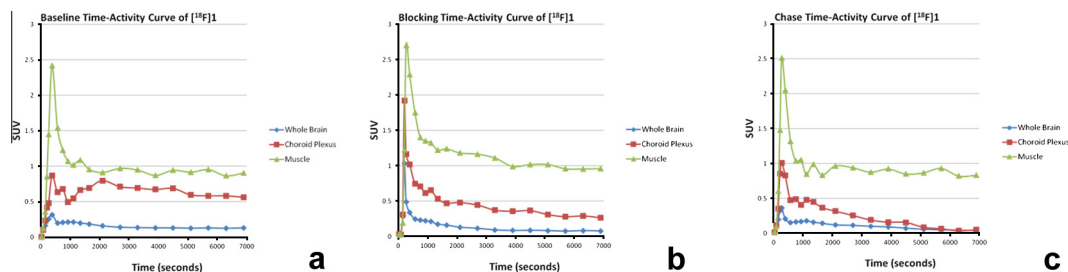


Figure 6. Time–activity curves of $[^{18}\text{F}]\mathbf{1}$ in the whole brain, choroid plexus, and muscle tissue of a cynomolgus monkey during (a) baseline scan (b) blocking study with 5 mg/kg of $\mathbf{1}$ administered 30 min prior to 5 mCi of $[^{18}\text{F}]\mathbf{1}$ (c) chase study with 5 mg/kg of $\mathbf{1}$ administered 2700 s after $[^{18}\text{F}]\mathbf{1}$.

has high densities of OTR in the nucleus accumbens.¹⁹ Therefore, we will be conducting future investigations utilizing the common marmoset as the model system. We will continue to perform struc-

ture/activity studies with derivatives of this candidate compound to increase brain penetration, increase affinity for OTR will maintaining selectivity, and eliminate binding to the cerebral ventricles.

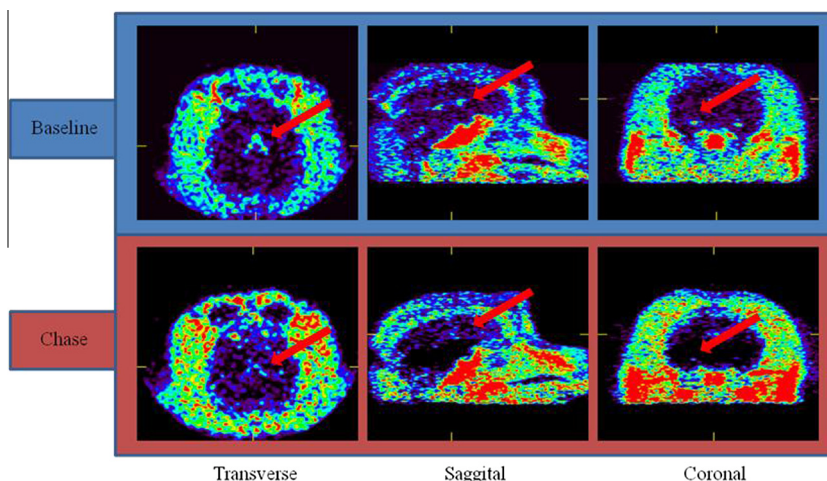


Figure 7. Images from 5 mCi of [^{18}F]**1** in a cynomolgus monkey model during the sum of the last 30 min of a 2 h baseline scan (blue) and the last 30 min of a chase study in which 5 mg/kg of **1** was administered 45 min after injection of 5 mCi of [^{18}F]**1** (red). The images demonstrate the removal of activity from the choroid plexus after administration of **1**.

Acknowledgements

We thank Larry Williams, Mel Camp and Eugene Malveaux for their contributions to the rodent studies. We thank the Yerkes National Primate Imaging Suite staff for their aid in performing non-human primate scans. We thank the NIMH PDSP directed by Bryan L. Roth M.D, Ph.D at the University of North Carolina at Chapel Hill and Project Officer Jamie Driscoll at NIMH, Bethesda MD, USA for their contributions of the human cell line studies. This research was funded by the National Institute of Mental Health through grant 5 R21 MH090776. We also acknowledge NIH MH064692 (L.J.Y.) and the National Center for Research Resources P51RR165 (currently P51OD11132) to YNPRC.

Supplementary data

Supplementary data associated with this article can be found, in the online version, at <http://dx.doi.org/10.1016/j.bmcl.2013.07.045>.

References and notes

- Duvigneaud, V.; Ressler, C.; Swan, J. M.; Roberts, C. W.; Katsoyannis, P. G. *J. Am. Chem. Soc.* **1954**, *76*, 3115.
- Ross, H. E.; Young, L. J. *Front. Neuroendocrinol.* **2009**, *30*, 534.
- Ross, H. E.; Freeman, S. M.; Spiegel, L. L.; Ren, X.; Terwilliger, E. F.; Young, L. J. *J. Neurosci.* **2009**, *29*, 1312.
- Donaldson, Z. R.; Young, L. J. *Science* **2008**, *322*, 900.
- Insel, T. R.; Winslow, J. T.; Wang, Z. X.; Young, L.; Hulihan, T. J. *Adv. Exp. Med. Biol.* **1995**, *395*, 227.
- Insel, T. R.; Shapiro, L. E. *Proc. Natl. Acad. Sci. U.S.A.* **1992**, *89*, 5981.
- Witt, D. M.; Winslow, J. T.; Insel, T. R. *Pharmacol. Biochem. Behav.* **1992**, *43*, 855.
- Young, L. J.; Winslow, J. T.; Wang, Z. X.; Gingrich, B.; Guo, Q. X.; Matzuk, M. M.; Insel, T. R. *Horm. Behav.* **1997**, *31*, 221.
- Young, L. J.; Lim, M. M.; Gingrich, B.; Insel, T. R. *Horm. Behav.* **2001**, *40*, 133.
- Young, L. J.; Wang, Z. *Nat. Neurosci.* **2004**, *7*, 1048.
- Insel, T. R.; O'Brien, D. J.; Leckman, J. F. *Biol. Psychiatry* **1999**, *45*, 145.
- Andari, E.; Duhamel, J. R.; Zalla, T.; Herbrecht, E.; Leboyer, M.; Sirigu, A. *Proc. Natl. Acad. Sci. U.S.A.* **2010**, *107*, 4389.
- Hollander, E.; Novotny, S.; Hanratty, M.; Yaffe, R.; DeCaria, C. M.; Aronowitz, B. R.; Mosovich, S. *Neuropsychopharmacology* **2003**, *28*, 193.
- Gregory, S. G.; Connelly, J. J.; Towers, A. J.; Johnson, J.; Biscocho, D.; Markunas, C. A.; Lintas, C.; Abramson, R. K.; Wright, H. H.; Ellis, P.; Langford, C. F.; Worley, G.; Delong, G. R.; Murphy, S. K.; Cuccaro, M. L.; Persico, A.; Pericak-Vance, M. A. *BMC Med.* **2009**, *7*, 62.
- Modi, M. E.; Young, L. J. *Horm. Behav.* **2012**, *61*, 340.
- Yamasue, H.; Yee, J. R.; Hurlmann, R.; Rilling, J. K.; Chen, F. S.; Meyer-Lindenberg, A.; Tost, H. *J. Neurosci.* **2012**, *32*, 14109.
- Meyer-Lindenberg, A.; Domes, G.; Kirsch, P.; Heinrichs, M. *Nat. Rev. Neurosci.* **2011**, *12*, 524.
- Loup, F.; Tribollet, E.; Dubois-Dauphin, M.; Dreifuss, J. J. *Brain Res.* **1991**, *555*, 220.
- Schorscher-Petcu, A.; Dupre, A.; Tribollet, E. *Neurosci. Lett.* **2009**, *461*, 217.
- Young, L. J.; Huot, B.; Nilsen, R.; Wang, Z.; Insel, T. R. *J. Neuroendocrinol.* **1996**, *8*, 777.
- Ebstein, R. P.; Knafo, A.; Mankuta, D.; Chew, S. H.; Lai, P. S. *Horm. Behav.* **2012**, *61*, 359.
- Smith, A. L.; Freeman, S. M.; Stehouwer, J. S.; Inoue, K.; Voll, R. J.; Young, L. J.; Goodman, M. M. *Bioorg. Med. Chem.* **2012**, *20*, 2721.
- Smith, A. L.; Freeman, S. M.; Voll, R. J.; Young, L. J.; Goodman, M. M. *Bioorg. Med. Chem. Lett.* **2013**, *23*, 902.
- Waterhouse, R. N. *Mol. Imaging Biol.* **2003**, *5*, 376.
- Disclosure: All animal experiments were carried out according to protocols approved by the Institutional Animal Care and Use Committee (IACUC) and Environmental Health and Safety Office of Emory University.
- Nilsson, C.; Lindvall-Axelsson, M.; Owman, C. *Brain Res. Brain Res. Rev.* **1992**, *17*, 109.
- Hirvonen, J.; Kreisl, W. C.; Fujita, M.; Dustin, I.; Khan, O.; Appel, S.; Zhang, Y.; Morse, C.; Pike, V. W.; Innis, R. B.; Theodore, W. H. *J. Nucl. Med.* **2012**, *53*, 234.
- Kreisl, W. C.; Liow, J. S.; Kimura, N.; Seneca, N.; Zoghbi, S. S.; Morse, C. L.; Herscovitch, P.; Pike, V. W.; Innis, R. B. *J. Nucl. Med.* **2010**, *51*, 559.
- Toloczko, D. M.; Young, L.; Insel, T. R. *Ann. N. Y. Acad. Sci.* **1997**, *807*, 506.